Review

Not peer-reviewed version

Amp-TB2 Protocol and Its Application to Amphiboles from Recent, Historical and Pre-historical Eruptions of Bezymianny Volcano, Kamchatka

Filippo Ridolfi *, Renat Almeev , Alexey Yu Ozerov , Francois Holtz

Posted Date: 30 September 2023

doi: 10.20944/preprints202309.2133.v1

Keywords: amphibole; thermobarometry; equilibrium crystallization; volcanoes; magma chamber; magma feeding system; seismic tomography

Review

Amp-TB2 Protocol and Its Application to Amphiboles from Recent, Historical and Pre-historical Eruptions of Bezymianny Volcano, Kamchatka

Filippo Ridolfi [1,*], Renat R. Almeev [1], Alexey Yu Ozerov [2] and Francois Holtz [1]

[1] Leibniz Universität Hannover ,Institut für Mineralogie, Callinstrasse 3, Hannover, 30167, Germany; filippo.ridolfi@uniurb.it;
[2] Institute of Volcanology and Seismology, Piip Boulevard 9, Petropavlovsk-Kamchatsky, 683006, Russia
* Correspondence: filippo.ridolfi@uniurb.it

Abstract: This article reports a protocol on the application of Amp-TB2 (single-amphibole thermobarometry; [1]) based on detailed electron microprobe analyses performed on homogeneous natural standards and synthetic glasses, and amphibole crystals (mostly phenocrysts) of volcanic products erupted by Bezymianny volcano during its activity through time. The application of this protocol is facilitated by a new version of the model (Amp-TB2.1.xlsx) including an equation to identify heterogeneous domains (disequilibrium; not suitable for thermobarometric constraints) and homogenous (equilibrium) zones within amphibole crystals, which can be used to quantify the physico-chemical parameters (i.e., pressure, P; temperature, T; volatile content in the melt, H_2O_{melt}; oxygen fugacity, fO_2) of "steady-state" magmatic crystallization. Application examples of the protocol, showing detailed core-rim microprobe data and physico-chemical parameter variations in representative amphibole phenocrysts of Bezymianny are also reported. The depth (and P) estimated by Amp-TB2.1 for this volcano are compared to seismic tomography results. Amp-TB2.1 results mainly shows (1) that Bezymianny is characterized by a very dynamic feeding system where the magma is stored at shallow crustal levels before recent activity periods characterized by climatic events and (2) that the pre-eruptive depth of magma storage generally increases with the age of the investigated products.

Keywords: amphibole; thermobarometry; equilibrium crystallization; volcanoes; magma chamber; magma feeding system; seismic tomography

1. Introduction

Amp-TB2 is a single-phase thermobarometric model for estimating the physico-chemical crstallization conditions of Ca- and Mg-rich amphiboles (Amp) in calc-alkaline and alkaline igneous rocks, across a wide P-T range (up to 2200 MPa and 1130 °C) and with relatively low uncertainties (P±12%, T±22°C, logfO_2±0.3, H_2O_{melt}±14%; [1]). It gives warnings whenever the input composition is incorrect or diverges from that of the calibration data and includes diagrams for an easy graphical representation of the results.

This model is the last of a series of thermobarometric applications where Ridolfi and co-authors progressively increased the accuracy and extended the validity of their thermobarometric formulations through the selection of consistent and "high-quality" experimental data and tested the capability of Amp to recover the physico-chemical conditions of "steady-state" (equilibrium) magmatic crystallization [2–7]. A "steady-state" condition of magma crystallization is meant as a nearly-stable magmatic environment where changes in intrinsic parameters, melt and mineral compositions that fall within the analytical and thermobarometric uncertainties. The main aim of Ridolfi and co-authors was to retrieve barometric equations capable to define crustal level magma

chambers of active and quiescent volcanoes and test their validity by comparing the estimated depths (and P) of magma reservoirs with those of complementary and independent methods such as seismicity and seismic tomography, e.g. [8–11].

[2] proposed the first single-Amp barometric and fO_2 equations valid for intermediate-basic magmas. These equations allowed to define the conditions and depth amplitude (from ca. 7 to 11 km) of the andesite magma chamber of El Reventador volcano, that started a new eruptive cycle in November 3 2002, after 26 years of quiescence, by the the intrusion of a basic magma at the base of the chamber (as inferred a 4.1magnitude volcano-tectonic earthquake with a hypocenterdepth of ~ 11 km on October 6 2002; [2,3].

[3] reported an overview of the crystallization of amphibole in calc-alkaline magmas and new single-Amp thermobarometric equations, including some testing with independent but complementary methodologies such as pre-eruptive seismicity (volcano-tectonic earthquake locations and frequency), seismic tomography, Fe–Ti oxides, amphibole–plagioclase, plagioclase–liquid equilibria thermobarometry and melt inclusion studies.

In 2012, Ridolfi and Renzulli tested previous Amp thermobarometers using "high-quality" experimental results (in which compositional data are provided with relatively low uncertanties and are consistent with the natural ones) obtained from calc-alkaline and alkaline starting materials and extended the validity of Amp-thermobarometry to alkaline magmas and P-T conditions up to 1130 °C and 2.2 GPa [4].

Other validations on the capability of Amp thermobarometry to recover the pressure (P) and depth of shallow magma chambers underneath active volcanoes are reported by independent reserchers, e.g. [12–19]. In addition, [7] published a mass-based method to obtain the formula parameters of Na, Na-Ca, Ca and oxo amphiboles from electron microprobe (EMP) analyses with a precision 2–4 times than that of classic Amp formula calculation approaches. The authors also attached an user friendly spreadsheet (AMFORM.xlsx) reporting warnings for bad analyses and large deviations from the ideal total element oxide and correct stoichiometry.

Some suggestions to avoid incorrect application of Amp thermobarometry, and thus avoiding unreliable results, are reported in [5,6]. In particular, these authors stated that intra-crystalline compositional and textural variations can be used to identify chemically homogeneous amphibole domains, indicative of "steady-state"magmatic crystallization, and to distinguish them from heterogeneous zones, resulting from disequilibrium crystallization or from element diffusion at the crystal-melt interface during magma mixing processes. However, the threshold between homogeneous and hetereogeneous domains in amphiboles measured by electron probe microanalysis (EPMA) and the extent at which Amp thermobarometry can be safely applied have not been fully defined. In addition, "apparent" heterogeneities in replicate measurements of originally homogeneous amphibole can be the result of uncertain analytical data (bad or loss of focusing during serial analyses, contamination from an adjacent phase, small inclusions that can not be easily identified, etc.)

In this work, we define a threshold between homogeneous and heterogeneous compositions and propose a protocol for the application of Amp-TB2 based on EPMA data of amphiboles from the recent, historical and pre-historical erupted products of Bezymianny volcano (Kamchatka), e.g. [20–25]. We show that the application of this protocol can lead to great details on the magma storage locations and processes, and their variations through time, underneath active volcanic plumbing systems.

2. Homogeneous vs. heterogeneous domains

2.1. Threshold between heterogeneous and homogeneous compositions as measured by EPMA

In order to find a criterion to exclude problematic analyses of amphibole and establish a threshold between homogeneous and heterogeneous compositional domains, we have performed multiple EPMA measurements (from 10 to 30 spot analyses) using a set of mineral and glass standards (Smithsonian Institution) and synthetic glasses with different composition, and calculated

Preprints (www.preprints.org) | NOT PEER-REVIEWED | Posted: 30 September 2023 doi:10.20944/preprints202309.2133.v1

the average amount of element oxides (element oxide in wt%), the relative standard deviation (σ, in wt%) and its percentage value (σ% = σ x 100/ element oxide wt%; Figure 1). Independently on the measured element oxide (i.e. SiO_2, TiO_2, Al_2O_3, Cr_2O_3, FeO_{tot}, MnO, MgO, CaO, Na_2O and K_2O), their averaged amount and EPMA setting (e.g., choice of analyzer crystals, current intensity and beam size) we found that σ% values decrease with the concentration of the measured element oxide (wt%) as follows:

$$\sigma\% = 5.7628 \times \text{element oxide wt\%}^{-0.661} \quad (R^2 = 0.8038) \qquad (1)$$

This relationship basically represents the averaged precision based on 10 measured oxides characterizing the quality of EPMA and degree of homogeneity of the used samples.

Figure 1 also shows the pattern of a curve equal to (1) multiplied by a factor of 2 (red broken curve), i.e.:

$$\sigma\% = 11.153 \times \text{element oxide wt\%}^{-0.661} \qquad (2)$$

It is worth to note that all measured homogeneous standards and glasses show σ% values ≤ to those calculated by equation (2) for all the measured element oxides. This relationship can then be used to distinguish homogeneous phases or intra-crystal domains from heterogeneous ones (see below).

In other words, homogeneous compositions should showσ% of all its element oxides lower than or equal to a threshold calculated by equation (2) whereas heterogeneous compositions are invariably characterized by higher uncertainties.

σ values calculated with (2) are 0.47 wt% at a level of measured element oxide of 70 wt%, 0.42 at 50wt%, 0.39 at 40 wt%, %, 0.31 wt% at 20 wt%, 0.24 wt% at 10 wt%, 0.19 wt% at 5 wt%, 0.14 wt% at 2 wt%, 0.11 wt% at 1 wt% and 0.05 wt% at 0.1 wt% levels. It is worth noting that (2) was recently used by [1] to select the "high-quality" dataset of experimental amphiboles for refining his Amp-TB2 model.

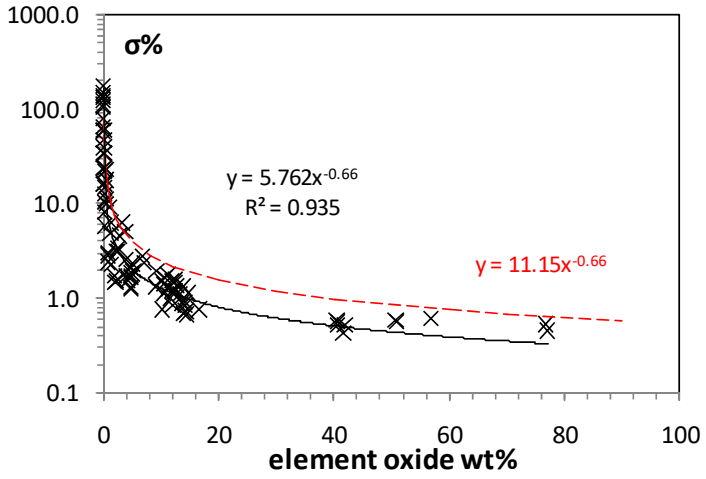

Figure 1. Correlation between the standard deviation percentage of different element oxides (σ% = σ x 100/ measured element oxide wt%) and the element oxide wt% of multiple EPMA measures (10–30 spot EMP analyses for each standard) on "homogeneous" Smithsonian microbeam standards (minerals and glasses: Kakanui hornblende 143965, Arenal hornblende NMNH 111356, Diopside NMNH 117733, Kakanui Augite NMNH 122142,VG-568 rhyolite NMNH 72854, VG-A99 basalt NMNH 113498-1; e.g. [26]) and glasses synthesized at 1600 °C and air conditions (i.e. high-K rhyolite, basaltic andesite and basalt) using the Cameca SX 100 of the University of Hannover with different EMP settings (black curve). The red broken curve reports this power relationship multiplied by a factor of 2. It shows that the mineral and glass samples, containing major oxides in a wide range, are characterized by lower value of σ%. Related equations are also reported with the same color.

 doi:10.20944/preprints202309.2133.v1

2.2. Intra-crystal analysis of Amp composition and related physico-chemical parameters

Figures 2–5 shows back scattered electron (BSE) images and core-rim intra-crystal EPMA profiles of representative amphibole phenocrysts from different eruptive products of Bezymianny volcano (see section 4 and Supplementary Material for additional information). Core-rim variations of physico-chemical parameters (i.e. pressure, P; temperature, T; oxygen fugacity expressed as difference from the Ni-NiO buffer, ΔNNO; volatile content in the melt, H_2O_{melt}) are also shown in all figures. These conditions were calculated with Amp-TB2 that is attached to this work in a modified version, including eq. 2 and an intra-crystal compositional analyses of the Bezymianny Amp phenocrysts in Figures 2–5. (i.e. Amp-TB2.1xlsx; Supplementary Material). Overall, the representative zoned phenocrysts show large compositional variations that are well above the homogeneity threshold provided by eq. 2. Nevertheless, in the core, mantle and rim zones of all phenocrysts, homogeneous intra-crystal domains (with σ%~≤ (2) for all measured element oxides) are found alternated to heterogeneous ones (with σ%> (2) for the main element oxides), indicating that Amp underwent stages of equilibrium ("steady-state") crystallization alternated by disequilibrium (kinetic) modifications (Supplementary Material).

Figure 2 reports the intra-crystal analysis of a phenocryst in the Amp-bearing andesite sample from the Novy lava dome in central crater of Bezymianny volcano (extruded in 1990). The phenocrysts looks apparently homogeneous in BSE imaging. However, EPMA indicates three homogeneous domains (core, mantle and rim) describing normal zoning, i.e.where the amount of Al_2O_3 (that is reversely correlated to SiO_2) and Na_2O decreases from core to rim, along with P (487±23, 374±13, 230±16 MPa), T (937±10, 910±8, 852±03 °C) and H_2O_{melt} (7.2±0.3, 6.6±0.1, 6.3±0.3 wt%), indicative of periods of magma stagnation ("steady-state" equilibrium crystallization) at three different crustal levels. MgO and FeO_{tot} variations go along with relative oxygen fugacity (ΔNNO, e.g. [2,27]) that is higher at the core (0.8±0.2 log units) and do not vary from mantle to rim (0.3±0.2 and 0.4±0.3 log units, respectively). In the heterogeneous zones, P, T and fO_2 roughly follow the pattern shown by the normal domains suggesting magma ascent. Nevertheless, values σ for Al_2O_3 and FeO_{tot} are much higher than those calculated with (2) and thus the phyisico-chemical parameters cannot be quantitatively constrained (Supplementary Material). The breakdown corona indicate that the phenocryst was brought at conditions outside the Amp stability field during its ascent to the surface.

Figure 3 shows the intra-crystal analysis of a twin phenocryst coming from another sample of the same lava dome extrusion. The BSE image shows evident zoning for the left side of the crystal with brightness progressively increasing towards the rim. Two homogeneous domains (core and rim) are easily distinguishable indicating different conditions (706±60 MPa, 971±13 °C, ΔNNO+2.2±0.4, 8.0±0.3 wt% H_2O_{melt} vs. 246±16 MPa, 874±7°C, ΔNNO+0.8±0.2 log units, 5.8±0.2wt% H_2O_{melt}) suggesting the ascent of the magma through the crust. Magma ascent is also suggested by the heterogeneous domain where the composition and phyisico-chemical parameters gradually vary from core to rim. However, σ% values calculated for this zone are much higher than (2) for Al_2O_3,FeO_{tot} and MgO, and P and logfO_2 standard deviations (20% and 0.9 log units) are well above those predicted by Amp-TB2 (12% and 0.4 log units, respectively; Supplementary Material). The gradual-diffusive compositional variation from core to rim could be due to a re-equilibration process in the crust by the contact with a more silicic melt, e.g. [28–31], or a constant-speed magma ascent where the Amp grew in contact with a melt gradually cooling down and evolving to silicic compositions.

Figure 4 shows an Amp phenocryst from the historical products of Bezymianny (1–1.35 kys BP, Lochmaty lava dome) with a very complex zoning. However, 4 homogeneous domains can be identified with the application of eq. 2 (core, mantle 1, mantle 2 and rim). Despite its complexity, Al_2O_3, TiO_2 and Na_2O do not show large variations from core to mantle 2 with calculated P-T-H_2O_{melt} conditions (543–603 MPa, 950–970°C, 7.2–7.3 wt%) varying well within the uncertainties of Amp-TB2. At the homogeneous rim zone slight decreases of P (498±26 MPa) and T (925±9 °C) come along with an increase of H_2O_{melt} (8.1±0.5 wt%). The main compositional variations are due to MgO and FeO_{tot} correlated with large fO_2 variations (core = -9.4±0.3, mantle 1 = -8.7±0.2, - mantle 2= 9.3±0.3, rim =

Preprints (www.preprints.org) | NOT PEER-REVIEWED | Posted: 30 September 2023 doi:10.20944/preprints202309.2133.v1

10.1±0.2 log units) (Supplementary Material). It is worth to note that the phenocryst does not show any breakdown rim and the calculated P goes down to 380 MPa at its rim (Figure 4). All of this suggests that the phenocryst grew in a magma zone at 400–600 MPa where its process of crystallization was affected by hot fluids/melts coming from deeper zones, and was finally rapidly ejected to the surface.

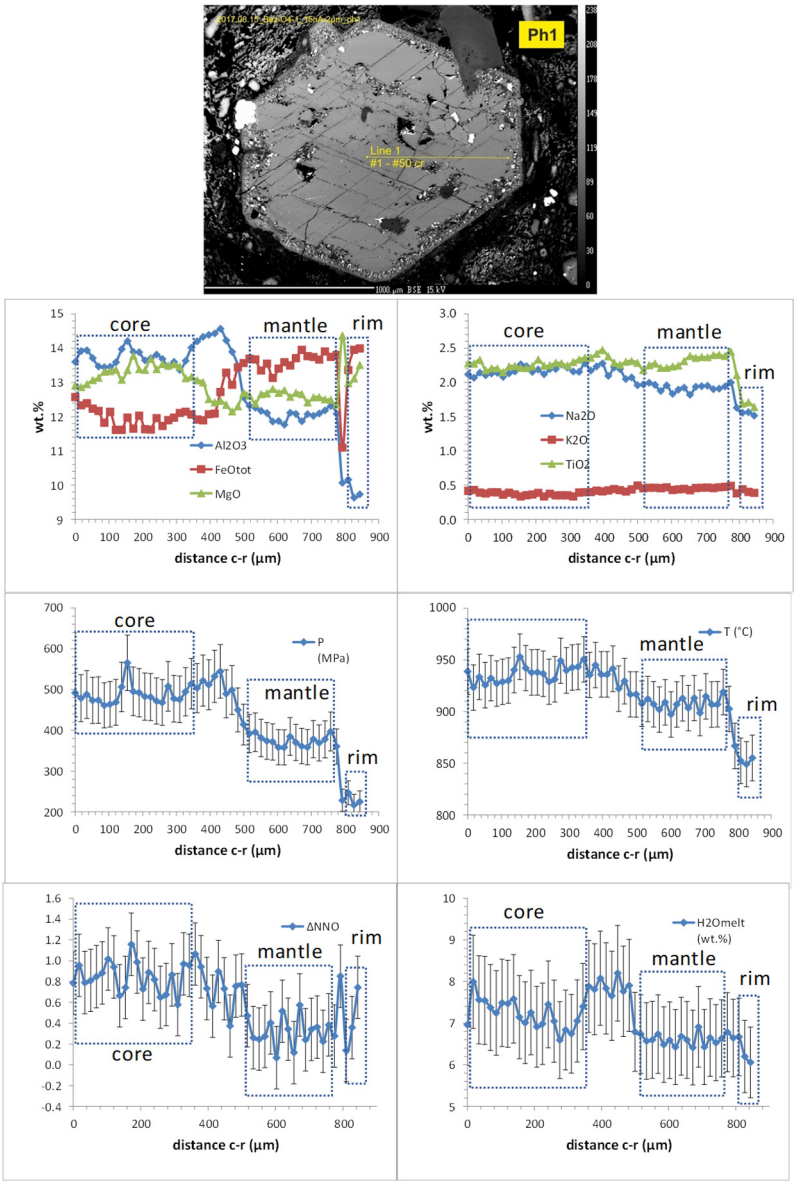

Figure 2. BSE image and core-rim quantitative EPMA profiles of an amphibole phenocryst from a Novydome 1990 extrusion (sample Bez O4-1). The phenocryst is characterized by a thin breakdown rim. The dashed boxes indicate compositionally homogeneous domains (i.e. σ% ~≤ 11.153 x element oxide wt%$^{-0.661}$,i.e. eq. 2) and reliable Amp-TB2 physico-chemical conditions (i.e. T σ ≤ 23 °C, P σ% ≤ 12%, ΔNNO σ ≤ 0.4, H_2O_{melt} σ% ≤ 14%). The bar errors in the T, P, ΔNNO and H_2O_{melt} vs. core-rime distance diagrams indicate these Amp-TB2 statistics uncertainties.

Preprints (www.preprints.org) | NOT PEER-REVIEWED | Posted: 30 September 2023 doi:10.20944/preprints202309.2133.v1

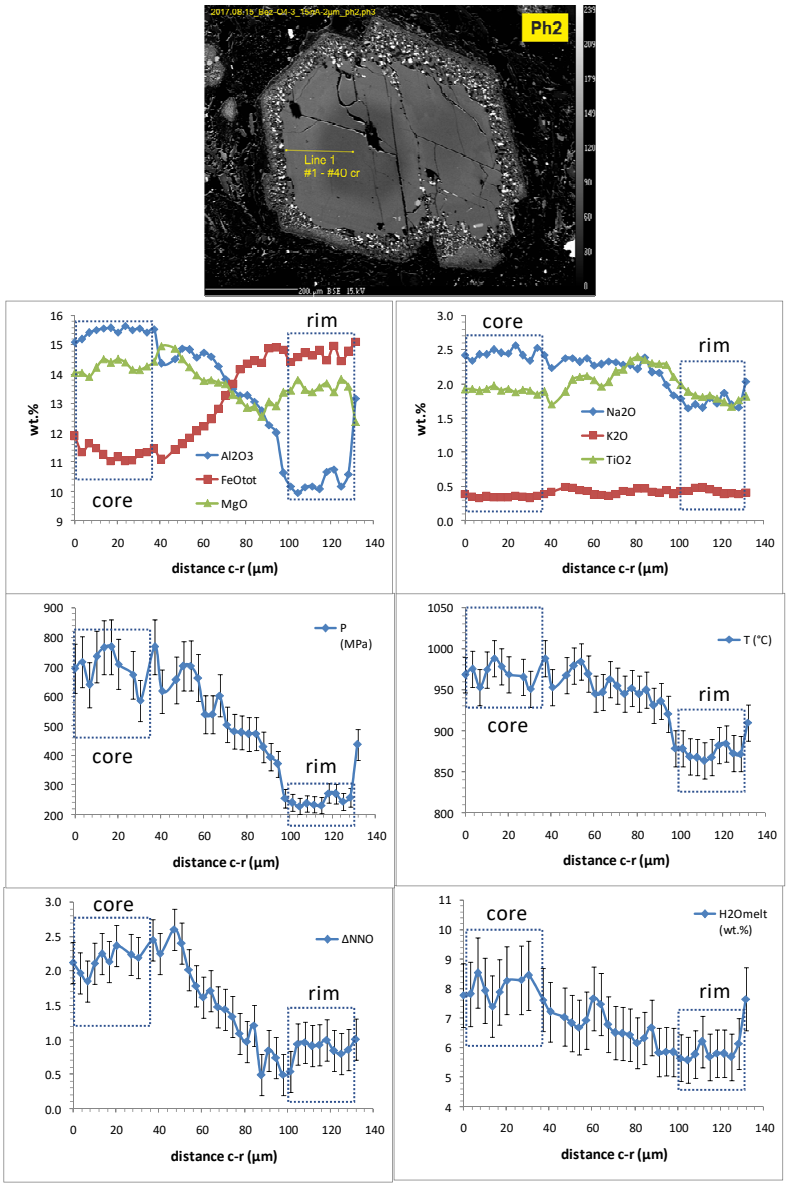

Figure 3. BSE image and core-rim quantitative EPMA profiles of an amphibole phenocryst from a Novy dome 1990 extrusion (sample Bez O4-3). The phenocryst is characterized by a thin breakdown rim. See Figure 2 for additional explanations.

Preprints (www.preprints.org) | NOT PEER-REVIEWED | Posted: 30 September 2023 doi:10.20944/preprints202309.2133.v1

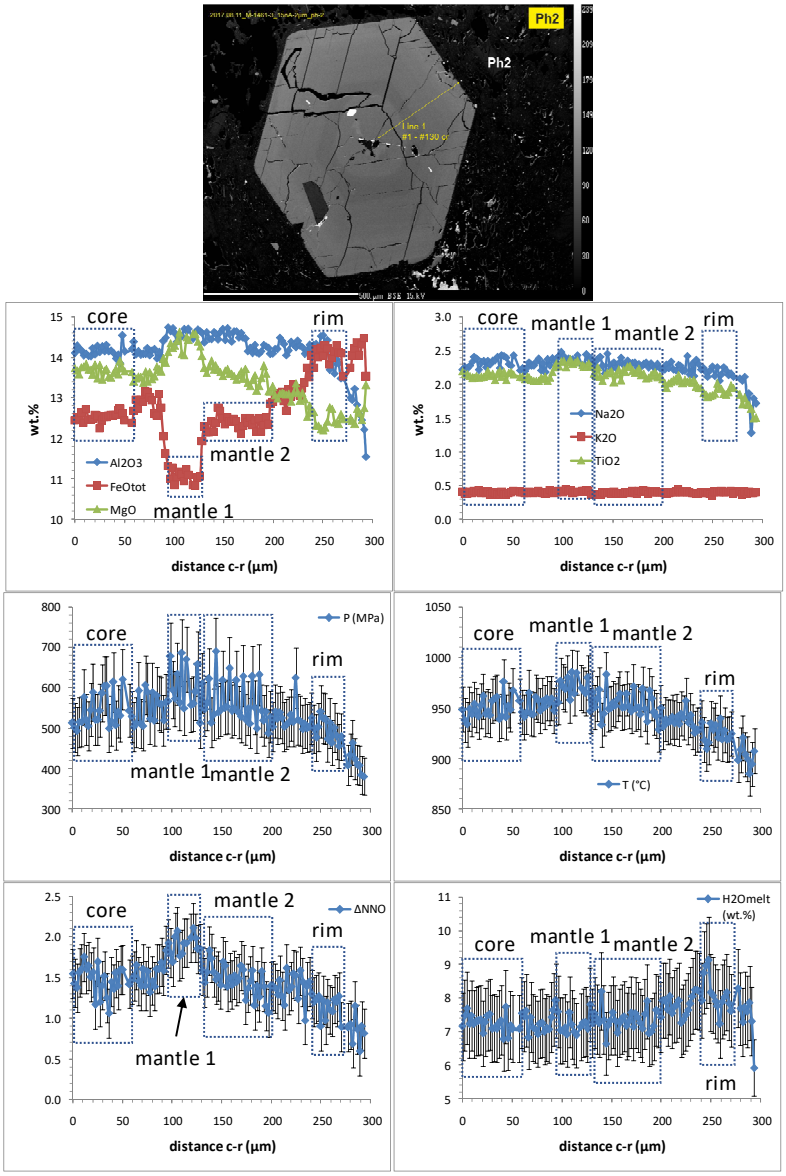

Figure 4. BSE image and core-rim quantitative EPMA profiles of an amphibole phenocryst from the lava dome Lokhmaty (sample M1461/3) extruded by Bezymianny volcano at 1–1.35 kys BP. It is worth to note that the phenocrysts do not show any sign of breakdown at its rim. See Figure 2 for additional explanations.

Figure 5 shows another Amp phenocryst characterized by complex zoning and no breakdown corona from the old historical products of Bezymianny (3.3–5.5 kys BP, lava dome Expeditsii). It is characterized by three homogeneous domains where Al_2O_3 increases reversely from core to rim 1 and decrease (normal zoning) from rim 1 to 2. This variation is accompanied by an increase of equilibrium P from 307±9 MPa (core) to 459±22 MPa (rim 1) followed by a decrease of ~100 MPa (rim 2 P = 379±13 MPa). [6] cautiously suggested to avoid the application of Amp thermobarometry to reverse zonings. However, this suggestion was due to the lack in their database of enough detailed core-rim EMP profiles. Reverse zonings are common in the recent and old products of Bezymianny and consistent with depth and size of the magma chambers obtained by seismic tomography (see [23] and section 4). A similar pattern is observed for H_2O_{melt} (core = 5.5, rim 1 = 7.2, rim 2 = 5.5±0.3 wt%). From core to rim 1, T follows the same pattern of P (894±7 and 936±9 °C, respectively) but do not show substantial variations at rim 2 (943±8 °C). ΔNNO shows a reverse relationship with P (core = 1.6±0.4, rim 1 = 1.2±0.2, rim 2 = 1.6±0.2 log units) (Supplementary Material; Figure 5). Al_2O_3 decreases at the heterogeneous domain to increase again towards rim 1. This patter suggest a process of interdiffusion of aluminium and should be not considered for thermobarometric constraints. All of this recalls for

Preprints (www.preprints.org) | NOT PEER-REVIEWED | Posted: 30 September 2023 doi:10.20944/preprints202309.2133.v1

a period of convective cycling of the magma within a crust chamber in between 460 and 310 MPa, followed by a rapid ejection to surface of the magma (as inferred by the absence of breakdown corona at the Amp phenocryst rim).

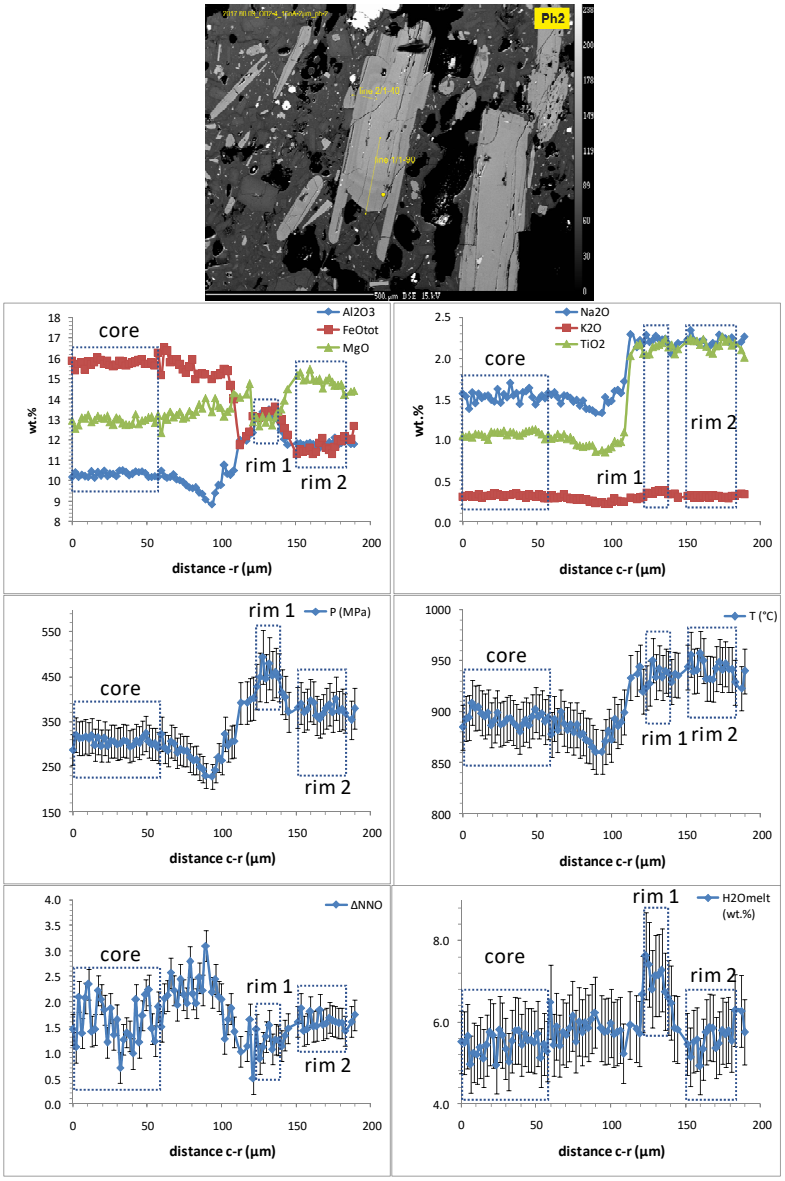

Figure 5. BSE image and core-rim quantitative EPMA profiles (line 1) of an amphibole phenocryst from the lava dome Expeditsii (Amp-bearing andesite, sample OB2/4) extruded by Bezymianny volcano at 3.3–5.5 kys BP. It is worth to note that the phenocrysts do not show any sign of breakdown at its rim. See Figure 2 for additional explanations.

3. Protocol on the application of Amp-TB2

This protocol is divided in three major steps which should be followed consecutively in order to fully exploit the capability of Amp to recover the magmatic processes and related phyisico-chemical variations and avoid misleading results.

3.1. Perform detailed EPMA profile

Independently on its igneous origin (plutonic vs. volcanic), detailed core-rim or rim-rim profile analyses through EPMA are highly recommended (e.g. Figures 2–5). Beam size and steps between the spot analyses should be as small as possible (typically 1 and 2 µm, respectively). Larger sizes

Preprints (www.preprints.org) | NOT PEER-REVIEWED | Posted: 30 September 2023 doi:10.20944/preprints202309.2133.v1

should be chosen as a compromise between the size and homogeneity of the crystals, previously characterized by high-quality BSE imaging (e.g. Figures 2–5). EPMA quantitative measurements must include Si, Ti, Al, Cr, Fe, Mn, Mg, Ca, Na and K. Particular EPMA settings are not required although a full characterization of Amp (including F and Cl) can be obtained following the procedure described in [26,32].

3.2. Check the quality of Amp composition

Before applying Amp-TB2.1, it is highly recommended to check the quality of the Amp compositions using AMFORM.xlsx, [7]. This is mostly done to prevent to bring low quality data in the following steps and avoid inaccuracies. Compositions showing incorrect initial and final TEO (total element oxides) and unbalanced stoichiometry should be discarded.

At this stage, it is convenient to input the compositional profiles into Amp-TB2.1 and perform a qualitative intra-crystal analysis by compositional, P, T, ΔNNO, H_2O_{melt} vs. profile distance diagrams (Figures 2–5). In additional, we also recommend to perform a last quality check. Indeed, although AMFORM.xlsx is a useful tool to avoid low quality data, it is worth noting that its calibration also includes Na-Ca, Na and oxo amphiboles and fail to distinguish small compositional variations due to the contamination of the EPMA measure by small inclusions of other phases (glass, fluids or other minerals) or by the occurrence of unpredictable current jumps at the analyzer crystals. For this reason, it is recommended to carefully check on the textural/compositional relationship within the Amp crystals and discard data randomly diverging from the common compositional variations in Amp (e.g. Figures 2–5).

3.3. Identify and quantify homgeneous domains with Amp-TB2.1

Homogeneous and heterogeneous domains can be identified graphically and using eq. (2) that is included in the new version of the model (Amp-TB2.1.xlsx; Supplementary Material). Other relevant changes in the new version, concern the last step of P calculation (i.e. xi; [1]) where P is determined by averaging Pb, Pc and Pd instead of P1a. This is due to minimize the high uncertainties of P1a (20%) that is highly sensitive to sodium and can result in unrealistically high P values when the quality of Na_2O analysis is low and/or occasional current jumps occur at the related EPMA analyzer crystal (typically TAP, e.g. [26]). Uncertainties of Amp-TB.1 as calculated on the experimental amphibole database (P±12%, T±23°C, ΔNNO±0.3, H_2O_{melt}±14%) are nearly identical to those of the older version [1]. Finally, average and standard deviation values must be calculated also for the physico-chemical parameter values given by the model in the zones constrained with eq. (2). σ and σ% values for the heterogeneous zones are generally higher than the uncertainties predicted by Amp-TB2.1. The physico-chemical parameters of these heterogeneous domains can not be quantitatively constrained. If an amphibole did not grow at "steady-state" (equilibrium) magmatic conditions or underwent high degrees of post-magmatic alteration it may not show any homogeneous domains. In this case, the calculated parameters do not have any qualitative and quantitative meaning. For homogeneous domains and unzoned amphiboles, σ and σ% must be ≤ to the uncertainties of the model. If these conditions are not verified, P1a should be manually inputted in the P cell for all the analyzed spots of the considereddomain, allowing Amp-TB2.xlsx to adjust the other physic-chemical parameters to the new input P. In this case P σ% should be ≤ to 20%.

Finally, the average and σ values obtained for each homogeneous domain can be plotted in the P-T, T-H_2O_{melt} and logfO_2-T diagrams in Amp-TB2 for a graphical representation and easy interpretation of the results (Figures 6 and 7; e.g. [5]).

4. The application of Amp-TB2.1 to Bezymianny amphiboles and comparison with seismic tomography results

Bezymianny volcano belongs to the Klyuchevskoy Group of volcanoes (Kamchatka, Russia) and it is the only volcano of the group which is characterized by the strong predominance of silicic eruptive products, that is a possible indication of the existence of large magmatic reservoir(s)

Preprints (www.preprints.org) | NOT PEER-REVIEWED | Posted: 30 September 2023 doi:10.20944/preprints202309.2133.v1

underneath the volcanic edifice where a parental basaltic magma differentiates to andesites and dacites [21–22,25,33–35]. Bezymianny volcano began growing approximately 10,000–11,000 yr BP, with periods of dormancy from 6900 to 4700 BP, 2750 to 2100 BP, 1550 to 1200 BP, and 1000 BP to 1955 AD. The pre-historic eruptive activity at Bezymianny formed extensive andesitic pyroclastic flow deposits and lava flows as well as andesitic to dacitic extrusive domes [36]. The latest eruptive cycle showed a reverse silicic to more mafic trend in the chemical composition of volcanic products; from dacite in 1956 to basaltic andesite in 2012 [22,35]. It has been argued that such acid-to-basic sequence observed in volcanic products is related to the existence of several interconnected magma chambers at different depths [22, 37]. These petrological observations were found to be consistent with independent geophysical data, e.g. [23,24,38,39]. Despite a large number of studies, the depth of magma chamber(s) underneath Bezymianny volcano is still an open question [20–22,25,34,35,37,40–43]. For example, [43] demonstrated that using compositional variations observed in Amp, the key mineral of Bezymianny volcanics, a full range of pressures from 200 to 900MPa can be recovered using older barometric formulation, i.e. [3]. However, these authors applied Amp thermobarometry only to some spot core and rim analyses, that do not allow to identify the complete intra-crystal compositional variations related with the evolution of the magma during Amp crystallization. Below we demonstrate, that much more details can be obtained on the evolution of P-T-conditions, if a detailed Amp compositional profiling and the filtering approach described above are performed.

Figures 6 and 7 summarize the results of the application of this protocol to amphiboles from the recent, historical and pre-historical products of Bezymianny volcano. These results are also reported in anExcel file in Supplementary Material. Amp compositions are from [22] who published EPMA data (mostly core-rim profiles) of 38 phenocrysts from the pre-climatic, climatic and post climatic deposits of the activity in 1955–2010. In addition, we performed new EPMA detailed profiles on selected 12 amphibole phenocrysts from Bezymianny products erupted in 1956 and 1990, and 35 Amp crystals from andesites with historical (1–1.35 kys and 3.3–5.5 kys BP) and pre-historical ages (older than 10 kys; from lava domes extruded before the formation of Bezymianny stratocone, i.e. 7.8 kys BP; ages are from [36]). These samples have been previously described in [43]. Amp compositions were measured using a Cameca SX100 microprobe (University of Hannover), operated at an accelerating voltage of 15 kV, 15 nA beam current with a beam spot of 2 μm for major elements (Supplementary Material). Na and K were analyzed first with counting times of 8 s. Counting time for other elements was 10 s on a peak and 5 s on background. Chlorine and fluorine were analyzed using a mode of second condition with similar beam spot but with a 40 nA beam current. Standards used for calibrations were oxides Fe_2O_3, Mn_3O_4, MgO, TiO_2, Cr_2O_3 and minerals – jadeite (Na), orthoclase (K), wollastonite (Si and Ca). NaCl and SrF2 were used to calibrate the halogens. In the course of each microprobe session, analytical accuracy was verified by measuring the Smithsonian Institution's Kakanui 143965 reference hornblende, e.g. [26].

In the following sections a summary of the main results and insights for the recent and old Amp-bearing products of Beziamianny is reported.

4.1. On the characteristic of the recent magma feeding system

Figure 6 reports the Amp-TB2.1 results for the recently erupted amphiboles, together with a tomography snapshot obtained from the Vp/Vs seismic analysis of earthquakes in a particularly active period of Bezymianny (i.e., 2005). Underneath Bezymianny, seismicity indicates the occurrence of a first magma zone (Magma Chamber 1) at depths 6–17 km (~160–530 MPa) and a second crustal high-Vp/Vs ratio zone (Magma Chamber 2) at 18–23 km depth (~560–690 MPa) that, due to its proximity with the first one, can also be interpreted as an extension of Magma Chamber 1. A lower crust-mantle source is shown underneath the nearby Klyuchevskoy volcano and most probably feeds both volcanoes, e.g. [23,24,44,45]. The occurrence of an extended magmatic zones (through Magma Chamber 1 and 2) is confirmed by our Amp-TB2.1 analysis (147–741 MPa) also showing Amp crystallization at "steady-state" conditions of 839–978 °C, 4.7–7.9 wt% H_2O_{melt} and fO_2 values from the NNO to 3 log units above. The lack of Amp-TB2.1 results at pressures of 290–360 MPa suggests the presence of two crustal chambers (Chamber A and B) connected by a narrower conduit. Figure 6

Preprints (www.preprints.org) | NOT PEER-REVIEWED | Posted: 30 September 2023 doi:10.20944/preprints202309.2133.v1

also shows normal and reverse zonings represented by dashed lines connecting physico-chemical conditions calculated for homogeneous domains. Reverse zonings are only found within the two chambers (i.e. at 147–286 and 358–741 MPa) while normal zonings can cross all the calculated P range (Figures 2 and 3). In addition, the amphiboles in the ash products before the climatic event of 1956 (pre-climatic) were directly ejected from the shallower Chamber A, as they only indicate equilibrium crystallization at 184–264 MPa and lowfO_2 values of NNO±0.2.The following products of the 1956 climatic event show a maximum Amp crystallization P of 589 MPa, well within Magma Chamber 2, while the post-climatic amphibole extend their equilibrium crystallization pressure (and depth) down to the top of Magma Source 3. It is worth to note that more recent products of Bezymianny (i.e. December 2017) indicate maximum Amp-TB2 depths well within this magma source at P of 850 MPa [25], comparable with depth of the MOHO transition. Oxygen fugacity and H_2O_{melt} show generally decreasing patterns from NNO+3 to NNO and 8.4 to 4.7 wt%, respectively, in agreement with experimental results of [21]. However, a few zonings for the deeper amphiboles in the post-climatic products show that H_2O_{melt} can decrease with both P and T, suggesting perturbation of the system from fluids or melts coming from deeper zones (Figure 6).

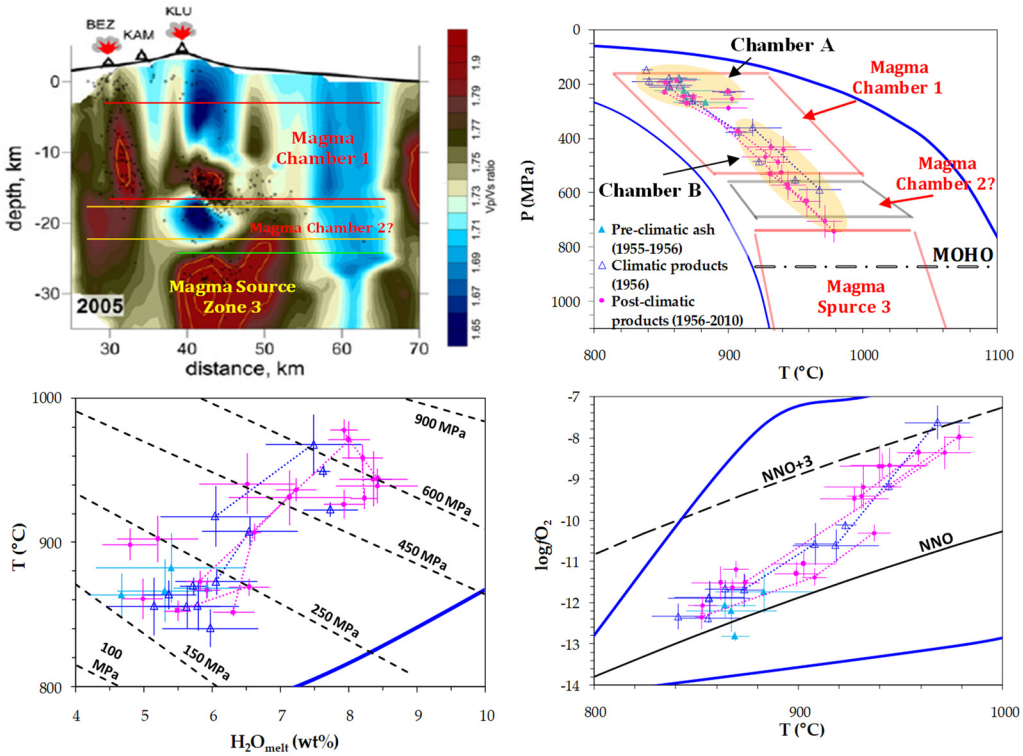

Figure 6. Comparison of a tomography seismic imaging for an active period of Bezymianny volcano (2005; image modified after [23] with Amp-TB2.1 results for the recent products (1955–2010). The depth-distance diagram (tomography image) shows a shallow crust magma chamber (1) underneath Bezymianny and a magma source (3) below Klyuchevskoy volcano characterized by high Vp/Vs values. Underneath Bezymianny another zone with relatively high Vp/Vsratios possible indicate the occurrence of a second magma chamber in the crust (Magma Chamber 2?) which can be arguably interpreted as an extension of Magma Chamber 1. The top of the Magma Chamber 1 is at 6 km, also postulated by [44] on the analysis of historical seismicity. These magma chambers are reported in the P-T diagram together with the MOHO (e.g. [45], also reporting two main storage regions where Amp crystallized at equilibrium conditions (Magma Chamber A and B; shaded-yellow fields). Depth-P conversion is calculated using a crust density of 2700 kg/m^3 from the top of the Bezymianny. In the P-T, T-H_2O_{melt} and logfO_2-T diagrams the dashed lines connect physico-chemical values calculated from homogeneous domains within the same crystals (normal or reverse zonings; Figures 2, 3 and 5). See [1] for additional explanations on the P-T, T-H_2O_{melt} and logfO_2-T diagrams.

 doi:10.20944/preprints202309.2133.v1

4.2. On the variation of the magma feeding system through ages

Figure 7 reports the results of the application of Amp-TB2.1 protocol for the historical and pre-historical products of Bezymianny. In the P-T diagram the locations of Magma Chamber 1 and 2 and Magma Source 3 are also reported for comparison, together with the MOHO transition. The first striking observation is that the depth of Amp crystallization is generally higher for these old products with a minimum calculated P (262 MPa) well within Magma Chamber 1, at the bottom of the shallower Chamber A identified by the recent amphiboles (cnf. Figures 6 and 7). This is observed only for the post-Bezymianny products (1–1.35 kys and 3.3–5.5 kys BP) while the minimum P of the amphiboles erupted before the genesis of the volcano (441 MPa) is located at the bottom of Magma Chamber 1 and within Chamber B identified for the recent products (cnf. Figures 6 and 7). Among the post-Bezymianny amphiboles, the younger ones (1–1.35 kys BP) mostly crystallized in the crust (261–603 MPa) and only one crystal testify the feeding of the system from a source located at the MOHO transition. The older ones (3.3–5.5 kys BP) show a continuous increase of crystallization depth down to the mantle (at 1273 MPa-1024°C) although large densities of data are observed in the range of 262–601 MPa (875–982°C) and at MOHO levels (853–963 MPa). The occurrence of the first magma storage region at crustal levels is supported by the P-T conditions calculated on cumulus-cognate Amp crystals (homogeneous and associated with other mafic mineral inclusions; e.g. [2]) found within these 3.3–5.5 kys old products (409–584 MPa; Figure 7). Amphiboles in the products preceding the genesis of Bezymianny (> 10 kys BP) show higher values of minimum and maximum crystallization pressure (441 and 1372 MPa, respectively). These amphiboles clearly show that the feeding system was characterized by a small crustal chamber at the base of Magma Chamber 1 (441–522 MPa) fed by a magma coming from a zone at crust-mantle transition (751–1056 MPa), in turn fed by deeper magmas (Figure 7).

Consistently with the recent Bezymianny amphiboles, reverse zonings are only found within the identified magma chambers while normal zonings can connect homogeneous domains crystallized at different magmatic zones. The T-H_2O_{melt} diagram shows a much more dispersed distribution than that of the recent amphiboles (cf. Figures 6 and 7) and zonings indicate that the amount of volatile in the melt increases with P-T only at shallow crustal depths (<400 MPa). At deeper levels, this trend is not observed and H_2O_{melt} can follow any directions between ideal isobaric and isothermal patterns (Figure 7). Relative oxygen fugacity (ΔNNO = 0.2–3.2 log units) shows a general increase with T, like for the recent amphiboles. It is however worth noting that values calculated at high depth conditions can lead to misleading results and interpretation as Amp-TB2.1 fO_2 equation was calibrated with experimental amphiboles synthesized at a maximum P of 700 MPa [21]. At lower pressure, the cumulus-cognate Amps are characterized by high fugacity values (NNO+3; Figure 7), suggesting that during stagnant periods the magma system releases to the surface most of its CO_2 cargo. Indeed, in the C-H-O fluid system fO_2 increases with the activity of H_2O, that is inversely related to the amount of CO_2, e.g. [43,27].

Preprints (www.preprints.org) | NOT PEER-REVIEWED | Posted: 30 September 2023 doi:10.20944/preprints202309.2133.v1

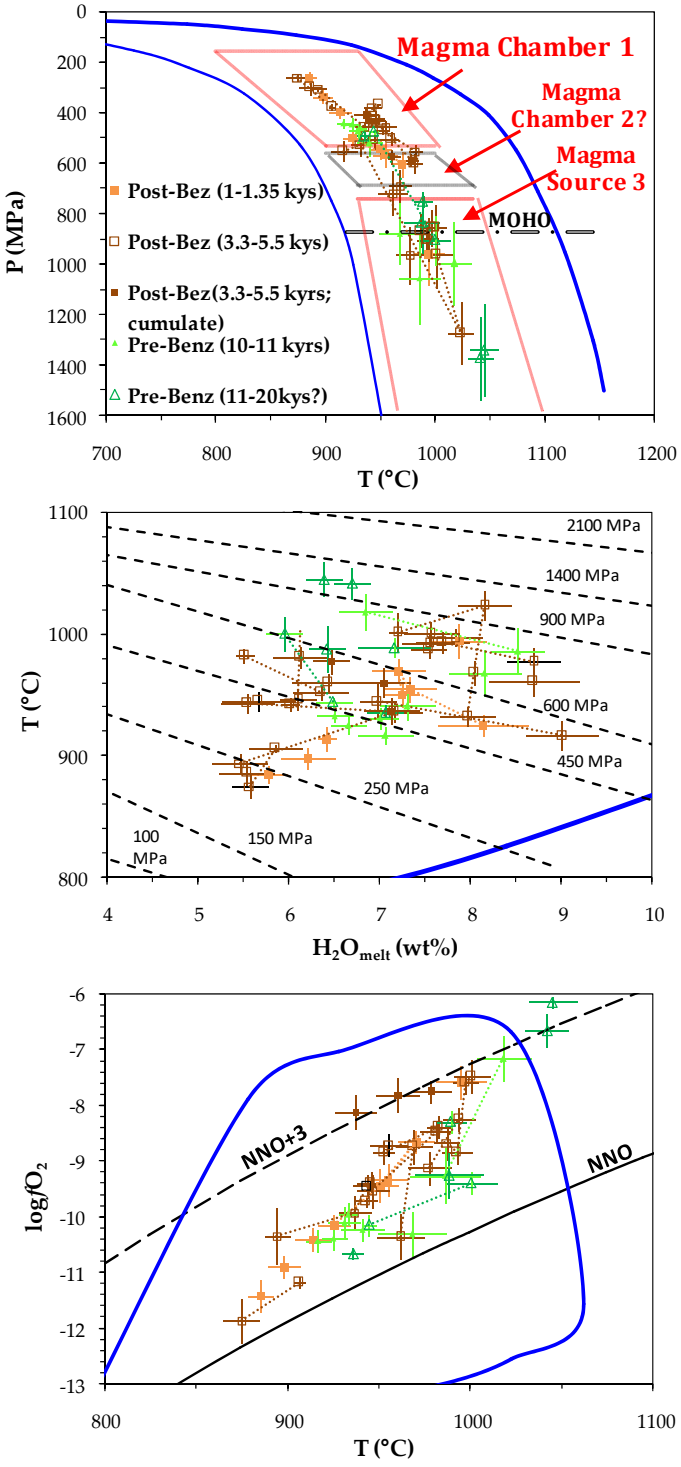

Figure 6. Amp-TB2 results for the historical and pre-historical amphiboles of Bezymianny volcano. Magma Chambers 1 and 2, and Source 3 are reported for comparison together with the MOHO (see Figure 6 caption). The dashed lines in the P-T, T-$H_2O_{melt}$and logfO_2-T diagrams connect physic-chemical values calculated from homogeneous zones within the same crystals (normal or reverse zonings; Figures 2, 3 and 5). All ages are related to the present time (BP). See [1] for additional explanations on the P-T, T-H_2O_{melt} and logfO_2-T diagrams.

4.3. Final remarks

Overall, the Amp-TB2.1 analysis of the recent, historical and pre-historical products of Bezymianny indicate a very dynamic feeding system changing frequently through time. The magma

is stored at shallow crust levels during recent activity periods and the depth of the magma withdraw by the volcano generally increases with the age. The recent amphiboles of Bezymianny indicates that the first explosive events after a period of quiescence are triggered by magmatic processes occurring at the shallower storage levels in the crust, similarly to other volcanoes, e.g. [2,3]. We suggest that in order to mitigate the volcanic risk, particular care should be taken in monitoring the seismicity of active volcanoes at these levels during quiescent periods (previously constrained through thermobarometry, petrology, geochemistry and geophysics). In particular, a rigorous application of the Amp-TB2 protocol can bring to clear definitions on the depth of these shallow-crust storage regions facilitating the interpretation of seismic volcano-tectonic events occurring underneath volcanoes, e.g. [2,3].

Supplementary Materials: The following supporting information can be downloaded at the website of this paper posted on Preprints.org.

Funding: This research was funded by the Alexander von Humboldt-Stiftung, with a research fellowship to the author, and the Deutsche Forschungsgemeinschaft (DFG), grant codesRI 3065/2-1 andRI 3065/2-2.

Data Availability Statement: Data supporting reported results can be found in the Supplementary Materials Amp-TB2.xlsx.

Acknowledgments: Holtz and many other scientists at the InstitutfürMineralogie at LUH are thanked for their support.

Conflicts of Interest: The authors declare no conflicts of interest.

References

1. Ridolfi, F. Amp-TB2: An Updated Model for Calcic Amphibole Thermo-barometry. *Minerals* **2021**, *11*, 32A.
2. Ridolfi, F.; Puerini, M.; Renzulli, A.; Menna, M.; Toulkeridis, T. The magmatic feeding system of El Reventador volcano (Sub-Andean zone, Ecuador) constrained by texture, mineralogy and thermobarometry of the 2002 erupted products. *J. Volcanol. Geotherm. Res.* **2008**, *176*, 94–106.
3. Ridolfi, F.; Renzulli, A.; Puerini, M. Stability and chemical equilibrium of amphibole in calc-alkaline magmas: An overview, new thermobarometric formulations and application to subduction-related volcanoes. *Contrib. Mineral. Petrol.* **2010**, *160*, 45–66.
4. Ridolfi, F.; Renzulli, A. Calcic amphiboles in calc-alkaline and alkaline magmas: Thermobarometric and chemometric empirical equations valid up to 1130 °C and 2.2 GPa. *Contrib. Mineral. Petrol.* **2012**, *163*, 877–895.
5. Ridolfi, F.; Renzulli, A.; Perugini, D.; Cesare, B.; Braga, R.; Del Moro, S. Unravelling the complex interaction between mantle and crustal magmas encoded in the lavas of San Vincenzo (Tuscany, Italy). Part I: Petrography and Thermobarometry. *Lithos***2016**, *244*, 218–232.
6. Gorini, A.; Ridolfi, F.; Piscaglia, F.; Taussi, M.; Renzulli, A. Application and reliability of calcic amphibole thermobarometry as inferred from calc-alkaline products of active geothermal areas in the Andes. *J. Volcanol. Geotherm. Res.* **2018**, *358*, 58–76.
7. Ridolfi, F.; Zanetti, A.; Renzulli, A.; Perugini, D.; Holtz, F.; Oberti, R. AMFORM, a new mass-based model for the calculation of the unit formula of amphiboles from Electron Micro-Probe analyses. *Am. Mineral.* **2018**, *103*, 1112–1125.
8. Benz, H.M.;Chouet, B.A.; Dawson, P.B.; Lahr, J.C.; Page, R.A.; Hole, J.A.Three-dimensional P and S wave velocity structure ofRedoubt Volcano, Alaska. *J.Geophys. Res.* **1996**, 101, 8111–8128.
9. Aspinal,W..P.; Miller, A.D.; Lynch, L.L.;Latchman, J.L.; Stewart, R.C.; White, R.A.; Power, J.A.Soufriére Hills eruption, Montserrat,1995–1997: volcanic earthquake locations and fault planesolutions. *Geophys. Res. Lett.* **1998**, 25, 3397–3400.
10. Lees, J.M. Seismic tomography of magmatic systems.*J.Volcanol. Geotherm. Res.* **2007**, 16.
11. Moran, S.C.; Malone, S.D.; Qamar, A.I.; Thelen, W.; Wright, A.K.; Caplan-Auerbach, J.Seismicity associated with renewed domebuildingat Mount St. Helens, 2004–2005. In *A volcano rekindled: the renewederuption of Mount St. Helens, 2004–2006,* 1st ed.; Sherrod, D.R.; Scott, W.E.; Stauffer, P.H., Eds.; U.S.GeologicalSurvey Professional Paper:USA, 2008, Volume 1; Chapter 2; pp.27-60.
12. Innocenti, S.; del Marmol, M.-A.; Voight, B.; Andreastuti, S.; Furman, T. Textural and mineral chemistry constraints on evolution of Merapi Volcano, Indonesia. *J. Volcanol. Geotherm. Res.* **2013**, *261*, 20–37.
13. Trua, T.; Marani, M.; Barca, D. Lower crustal differentiation processes beneath a back-arc spreading ridge (Marsili seamount, Southern Tyrrhenian Sea). *Lithos***2014**, 190–191, 349-362.

14. Burns, D.H.; de Silva, S.L.; Tepley, F., III; Schmitt, A.K.; Loewen, M.W. Recording the transition from flare-up to steady-state arc magmatism at the Purico–Chascon volcanic complex, northern Chile. *Earth Plan. Sci. Lett.* **2015**, *422*, 75–86.
15. Harangi, S.; Novák, A.; Kiss, B.; Seghedi, I.; Lukács, R.; Szarka, L.; Wesztergom, V.; Metwaly, M.; Gribovszki, K. Combined magnetotelluric and petrologic constrains for the nature of the magma storage system beneath the Late Pleistocene Ciomadul volcano (SE Carpathians). *J. Volcanol. Geotherm. Res.* **2015**, *290*, 82–96.
16. Dobretsov, N.L.; Simonov, V.A.; Koulakov, I.Y.; Kotlyarov, A.V. Migration of fluids and melts in subduction zones and general aspects of thermophysical modeling in geology. *Rus. Geol. Geophys.* **2017**, *58*, 571–585.
17. Mata, J.; Martins, S.; Mattielli, N.; Madeira, J.; Faria, B.; Ramalho, R.S.; Silva, P.; Moreira, M.; Caldeira, R.; Moreira, M.; et al. The 2014-15 eruption and the short-term geochemical evolution of the Fogo volcano (Cape Verde): Evidence for small-scale mantle heterogeneity. *Lithos* **2017**, *288–289*, 91–107.
18. Nagasaki, S.; Ishibashi, H.; Suwa, Y.; Yasuda, A.; Hokanishi, N.; Ohkura, T.; Takemura, K. Magma reservoir conditions beneath Tsurumi volcano, SW Japan: Evidence from amphibole thermobarometry and seismicity. *Lithos* **2017**, *278–281*, 153–165.
19. Stechern, A.; Just, T.; Holtz, F.; Blume-Oeste, M.; Namur, O. Decoding magma plumbing and geochemical evolution beneath the Lastarria volcanic complex (Northern Chile)—Evidence for multiple magma storage regions. *J. Volcanol. Geotherm. Res.* **2017**, *338*, 25–45.
20. Almeev, R.R.;Ariskin, A.A.;Ozerov, A.Y.; Kononkova, N.N.. Problems of the stoichiometry and thermobarometry of magmatic amphiboles: an example of hornblende from the andesites of Bezymianny volcano, Eastern Kamchatka. *Geochem. Intern.* **2002**, *40*, 723-738.
21. Almeev, R.R.; Holtz, F.; Ariskin, A.A.; Limura, J.-I. Storage conditions of Bezymianny Volcano parental magmas: Results of phase equilibria experiments at 100 and 700 MPa. *Contrib. Mineral. Petrol.* **2013**, *166*, 1389–1414.
22. Turner, S.J.; Izbekov, P., Langmuir, C. The magma plumbing system of Bezymianny Volcano: Insights from a 54 year time series of trace element whole-rock geochemistry and amphibole compositions. *J. Volcanol. Geotherm. Res.* **2013**, *263*, 108–121.
23. Koulakov, I.; Gordeev, E.I.;Dobretsov, N.L.;Vernikovsky, V.A.;Senyukov, S.;Jakovlev, A.;Jaxybulatov, K. Rapid changes in magma storage beneath the Klyuchevskoy group of volcanoes inferred from time-dependent seismic tomography. *J. Volcanol. Geotherm. Res.* **2013**, *263*, 75–91.
24. Koulakov, I.;Abkadyrov, I.; Al Arifi, N.;Deev, E.;Droznina, S.; Gordeev, E.I.;Jakovlev, A.; El Khrepy, S.;Kulakov, R.I.;Kugaenko, Y.;Novgorodova, A.;Senyukov, S.; Shapiro, N.;Stupina, T.; West, M. Three different types of plumbing system beneath the neighboring active volcanoes of Tolbachik,Bezymianny, and Klyuchevskoy in Kamchatka. *J. Geophys. Res.: Solid Earth* **2017**, *122*, 3852-3874.
25. Davydova, V.O.;Shcherbakov, V.D.;Plechov, P.Yu.;Koulakov, I.Yu. Petrological evidence of rapid evolution of the magma plumbing systemofBezymianny volcano in Kamchatka before the December 20th,2017 eruption. *J. Volcanol. Geotherm. Res.* **2022**, *421*, 107422.
26. Liu, Y.; Yang, W.; Zhang, C.; Bao, Z.; Wu, S.; Almeev, R.A.; Ridolfi, F.;Oberti, R. New Compositional and Structural Constraints on theSmithsonian Microanalytical Reference Materials: AmphibolesfromKakanui and Arenal. *Geostand. Geoanal. Res.* **2023**, 47, 595-608.
27. Scaillet, B.; Evans, B.W. The 15 June 1991 eruption of MountPinatubo; I, Phase equilibria and pre-eruption P-T-fO_2-fH_2conditions of the dacite magmas. *J Petrol* **1999**,*40*, 381–411.
28. Chakraborty, S. Rates and mechanisms of Fe-Mg interdiffusion in olivine at 980°–1300° C. *J. Geophys. Res.: Solid Earth* **1997**, *103*, 12317-12331.
29. Costa, F.; Chakraborty, S.; Dohmen, R. Diffusion coupling between trace and major elements and a model for calculation of magma residence times using plagioclase. *Geochem. Cosmochem. Acta* **2003**, *67*, 2189-2200.
30. Costa, F.; Dohmen, R.; Chakraborty, S. Time scales of magmatic processes from modeling the zoning patterns of crystals. *Rev. Mineral. Geochem.***2008**, *69*, 545-594.
31. Costa, F.; Shea, T., Ubide, T. Diffusion chronometry and the timescales of magmatic processes. *Nature Rev. Earth Environ.* **2020**,*1*, 201-214.
32. Zhang, C.; Koepke, J.; Wang, L.-X.; Wolff, P.E.; Wilke, S.; Stechern, A.; Almeev, R.A.; Holtz, F. A Practical Method for Accurate Measurement of Trace Level Fluorine in Mg- and Fe-Bearing Minerals and Glasses Using Electron Probe Microanalysis. *Geostand. Geoanal. Res.* **2016**, 40, 351-363.
33. Bogoyavlenskaya, G.E.; Braitseva, O.A.; Melekestsev, I.V.; Maksimov AP, Kiriyanov, V.Xu.; Dan Miller, C. Catastrophic eruptions of the directed-blast type at Mount St. Helens, bezymianny and Shiveluch volcanoes. *J Geodyn.* **1985,** *3*, 189-218.
34. Ozerov, A.A.; Ariskin, A.A.; Kyle, P.; Bogoyavlenskaya, G.E.; Karpenko, S.F. Petrological-geochemical model for genetic relationshipsbetween basaltic and andesitic magmatism of KlyuchevskoyandBezymianny volcanoes, Kamchatka. *Petrology* **1997**, *5*, 550–569.

35. Davydova, V.O.; Shcherbakov, V.D.; Plechov, P.Xu.; Perepelov, A.B. Petrology of mafic enclaves in the 2006–2012 eruptive products of Bezymianny Volcano, Kamchatka. *Petrology* **2017**, 25, 592–614.
36. Braitseva, O.A.; Melekestsev, I.V.; Bogoyavlenskaya, G.E.; Maksimov, A.P. Bezymianny: eruptive history and dynamics. *VolcanolSeismol* **1991**, 12, 165–195.
37. Shcherbakov, V.; Plechov, P.; Izbekov, P.; Shipman, J.Plagioclase zoning as an indicator of magma processes at BezymiannyVolcano, Kamchatka. *Contrib Mineral Petrol* **2011**,*162*, 3–99.
38. Koloskov, A.V.; Ananyev, V.V. New Data on the Age, Material Composition, and Geological Structure of the Central Kamchatka Depression (CKD). Part 2. The Mineralogical Composition of Volcanic Rocksand Mantle Xenoliths. Toward a Petrologic Model. *J. Volcanol. Seism.* **2020**, *14*, 145–165.
39. Koulakov, I.; Plechov, P.; Mania, R.; Walter, T.R.; Smirnov, S.Z.; Abkadyrov, I.; Jakovlev, A.; Davydova, V.; Senyukov, S.; Bushenkova, N.; Novgorodova, A.; Stupina, T.; Droznina, S.Ya. Anatomy of the Bezymianny volcano merely before an explosive eruption on 20.12.2017. *Sci. Rep.* **2021**,*11*, 1758.
40. Maksimov, A.P.;Kadik, A.A.;Korovushkina, E.Y.; Ivanov, B.V.. Crystallization of an andesite melt with a fixed water content at pressures up to 12 kbar. *Geochemistry International* **1978**, *15*, 20-29.
41. Plechov, P.; Tsai, A.; Shcherbakov, V.; Dirksen, O.. Opacitization conditions of hornblende in Bezymyannyi volcano andesites (March 30, 1956 eruption). *Petrology* **2008**, *16*, 19-35.
42. Shcherbakov, V.D.; Neill, O.K.;Izbekov, P.E.;Plechov, P.Y.. Phase equilibria constraints on pre-eruptive magma storage conditions for the 1956 eruption of Bezymianny Volcano, Kamchatka, Russia. *J. Volcanol. Geotherm. Res.* **2013**, *263*, 132-140.
43. Almeev, R.R.; Kimura, J.-I.;Ariskin, A.A.;Ozerov, A.Y.. Decoding crystal fractionation in water-rich calc-alkaline magma from Bezymianny volcano, Kamchatka, Russia, using mineral and bulk rock chemistry. *J. Volcanol. Geotherm. Res.* **2013**, *263*, 141–171.
44. Thelen, W.; West, M.; Senyukov, S. Seismic characterization of the fall 2007 eruptive sequence at Bezymianny Volcano, Russia. *J. Volcanol. Geotherm. Res.* **2010**, *194*, 201-213.
45. William, B.F.; Shapiro, N.M.; Gusev, A.A. Progressive reactivation of the volcanic plumbing system beneath Tolbachik volcano (Kamchatka, Russia) revealed by long-period seismicity. *Earth Plan. Sci. Lett.* **2018**, *493*, 47–56.